

## The essential light chain is required for full force production by skeletal muscle myosin

PETER VANBUREN\*, GUILLERMINA S. WALLER†, DAVID E. HARRIS‡, KATHLEEN M. TRYBUS†, DAVID M. WARSHAW‡§, AND SUSAN LOWEY†

Departments of †Molecular Physiology and Biophysics, and \*Cardiology, University of Vermont, Burlington, VT 05405; and ‡Rosenstiel Basic Medical Sciences Research Center, Brandeis University, Waltham, MA 02254

Communicated by William P. Jencks, September 14, 1994 (received for review July 11, 1994)

**ABSTRACT** Myosin, a molecular motor that is responsible for muscle contraction, is composed of two heavy chains each with two light chains. The crystal structure of subfragment 1 indicates that both the regulatory light chains (RLCs) and the essential light chains (ELCs) stabilize an extended  $\alpha$ -helical segment of the heavy chain. It has recently been shown in a motility assay that removal of either light chain markedly reduces actin filament sliding velocity without a significant loss in actin-activated ATPase activity. Here we demonstrate by single actin filament force measurements that RLC removal has little effect on isometric force, whereas ELC removal reduces isometric force by over 50%. These data are interpreted with a simple mechanical model where subfragment 1 behaves as a torque motor whose lever arm length is sensitive to light-chain removal. Although the effect of removing RLCs fits within the confines of this model, altered crossbridge kinetics, as reflected in a reduced unloaded duty cycle, probably contributes to the reduced velocity and force production of ELC-deficient myosins.

A simple structural model that could account for the movement of actin by the molecular motor myosin was first proposed by H. E. Huxley in 1969 (1). This "tilting cross-bridge" hypothesis suggested that the motor's power stroke is due to the myosin head rotating while bound to actin. When subsequent experiments failed to provide direct evidence that the globular portion of the myosin head undergoes an angular change, interest shifted to myosin's more distal neck region, which binds both the essential and regulatory light chains (LCs) (2). This LC-stabilized neck region consists of an 85-Å  $\alpha$ -helical stretch of amino acids (3), which may act as a rigid lever to power actin movement. Consistent with this modified tilting crossbridge model, removal of either or both LCs slowed the velocity at which skeletal muscle myosin moved actin in a motility assay (4). Here we further test the role of the LCs by using *in vitro* force measurements on single actin filaments (5) to assess how LC removal affects this fundamental property of the myosin motor.

### MATERIALS AND METHODS

**Proteins.** Myosin heavy chain devoid of both classes of LCs was prepared from chicken pectoralis skeletal muscle myosin (4). In brief, myosin was incubated in 4.7 M  $\text{NH}_4\text{Cl}$  and applied to a Superose 6 gel filtration column (FPLC; Pharmacia) to separate the free LCs from the heavy chain. To form myosin having only one of its LCs, the heavy chain was incubated with either regulatory LC (RLC) or essential LC (ELC). As a control, myosin having its full complement of LCs was prepared by incubation with both LC species

(TLC-myosin). Unbound LC was removed by precipitation of the reconstituted myosin.

**Force Measurements.** To determine the effect of LC removal on myosin force production, we used a technique (5) for measuring force in the motility assay as developed by Kishino and Yanagida (6). The myosin was first adhered as monomers to a nitrocellulose-coated coverslip. A single fluorescently labeled actin filament was then attached by means of *N*-ethylmaleimide-modified skeletal muscle myosin to the tip of a calibrated, ultracompliant glass microneedle. As the free end of the actin filament interacted with myosin on the nitrocellulose surface, the deflection of the microneedle was recorded on video. The video images were digitized in order to compute myosin's maximum steady-state force from the microneedle's deflection and stiffness. Force data were normalized to the length of actin filament interacting with the surface-bound myosin. The slope of the regression through these data (i.e., maximal force per unit length of actin) is proportional to the average force per crossbridge (5). The velocity of freely moving actin filaments was determined by computer (7, 8). Velocities are reported as the mean and standard deviation for at least 18 filaments. Actin filament motility and force were recorded in low-salt (25 mM KCl) assay buffer at 30°C (5).

The following procedure was performed to rebind ELCs to ELC-deficient myosin previously adhered to the nitrocellulose surface. The adherent ELC-deficient myosin was incubated on ice for 30 min with a solution containing ELC at 100  $\mu\text{g}/\text{ml}$  in 300 mM KCl/5 mM  $\text{MgCl}_2$ /25 mM imidazole/1 mM EGTA/10 mM dithiothreitol/0.05% bovine serum albumin, pH 7.4. The remaining preparative steps required for actin filament motility were then completed (5).

**Duty Cycle.** To assess the possible effects of LC removal on crossbridge cycle kinetics, unloaded duty cycle, defined as the fraction of the total crossbridge cycle that myosin spends attached to actin in a motion generating state, was estimated (9, 10). The velocity of freely moving actin filaments was measured over a sparsely coated myosin surface prepared by adding myosin at 15  $\mu\text{g}/\text{ml}$  to the microchamber.  $\text{NH}_4^+$ /EDTA-ATPase activities of surface-bound myosin were compared with those of known amounts of myosin in solution to determine the surface density of myosin and, thus, the number of myosin heads available to interact with a unit length of actin filament. Motility data were plotted as actin filament velocity ( $V$ ) versus the number of myosin heads ( $N$ ) available to interact with an actin filament (see Fig. 4B). These data were fitted to the stochastic equation  $V = (a \times V_{\text{max}}) \times [1 - (1 - f)^N]$ , where the duty cycle ( $f$ ) and the efficiency of motion transmission ( $a \times V_{\text{max}}$ ) are parameters of the fit.

The publication costs of this article were defrayed in part by page charge payment. This article must therefore be hereby marked "advertisement" in accordance with 18 U.S.C. §1734 solely to indicate this fact.

Abbreviations: LC, light chain; ELC, essential LC; RLC, regulatory LC; TLC-myosin, myosin with its total LC (ELC and RLC) complement; S1 and S2, myosin subfragments 1 and 2.

§To whom reprint requests should be addressed.

**Lever Arm Model.** A crossbridge model first proposed by Huxley and Simmons (11) was adapted as a means of interpreting the observed effects of LC removal on myosin force and motion generation. The choice of this model is not exclusive, but it does provide a framework for predicting the relationship between the structural and mechanical properties of myosin.

Rayment *et al.* (3) have shown that the myosin head (subfragment 1, S1) consists of a motor domain from which extends a long LC-stabilized  $\alpha$ -helix. This neck region may serve as a rigid lever of length  $l$ , through which small displacements that occur in the motor domain are amplified (Fig. 1). By incorporating this crucial assumption into the Huxley and Simmons crossbridge model, the force ( $F_{\text{uni}}$ ) at the lever's end is the result of stretching an elastic element within the myosin S2 segment as the crossbridge undergoes its working stroke from state 1 to state 2. Given that the S2 segment may not be required for force generation (6), modifications to the model may be required once a more precise location for this elasticity has been determined. The transition from state 1 to state 2 is assumed to result in a fixed maximum angular change (ref. 12;  $\phi_{\text{max}} = 45^\circ$ ). Even though the transition itself is assumed to be instantaneous, an average angular velocity can be calculated based on  $\phi_{\text{max}}$  and the average time spent in the strongly bound state. Therefore, unloaded actin filament velocity will be related to the product of the average angular velocity during the working stroke and the lever arm length. The maximum force of a single crossbridge ( $F_{\text{uni}}$ ) will be determined by the extent to which the elastic element of stiffness ( $k$ ) is stretched during the working stroke ( $l \sin \phi_{\text{max}}$ ); i.e.,  $F_{\text{uni}} = kl \sin \phi_{\text{max}}$ . The average force for a crossbridge population ( $F_{\text{avg}}$ ) is the product of  $F_{\text{uni}}$  and the proportion of attached crossbridges that undergo the transition to state 2 ( $n_2$ ) as follows:

$$F_{\text{avg}} = n_2 F_{\text{uni}}. \quad [1]$$

If LC removal collapses the neck region, then actin filament velocity would be linearly dependent on lever length (see Fig. 4A). However, force will be dependent on both lever arm length and the proportion of crossbridges that undergo the working stroke (Eq. 1), assuming that the S2 segment stiffness,  $k$ , and  $\phi_{\text{max}}$  are independent of LC removal.

The relationship between lever arm length and  $n_2$  can be predicted by using the Huxley and Simmons model (11). The probability that an attached crossbridge undergoes the working stroke is limited by the energy barrier imposed by

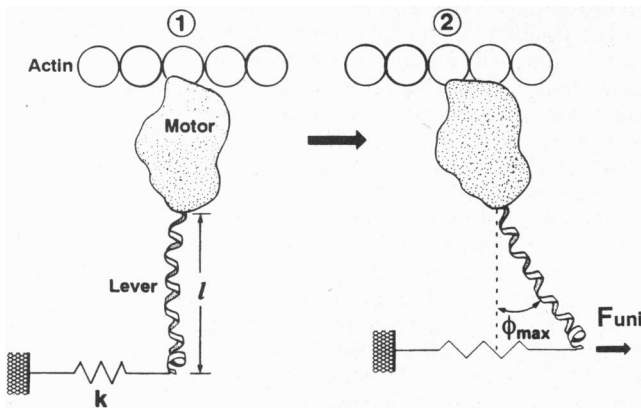


FIG. 1. Illustration depicting the mechanism of force generation as adapted from Huxley and Simmons (11). The  $\alpha$ -helical neck region (lever) is stabilized by the ELC at its amino terminus and the RLC in tandem. Force ( $F_{\text{uni}}$ ) is generated as the crossbridge undergoes a working stroke from state 1 to state 2. See *Materials and Methods* for a detailed description.

stretching of the elastic element. Therefore, if the extent of stretch is reduced for LC-deficient myosins due to a reduction in the lever arm length, then a greater proportion of attached crossbridges may undergo the working stroke. The resultant increase in  $n_2$  is analogous to the increase in  $n_2$  following a rapid release in muscle length at peak isometric force (11). Therefore, as predicted by Huxley and Simmons (equation 15 in ref. 11):

$$n_2 = 0.5[1 + \tanh(\alpha y/2)], \quad [2]$$

where  $\alpha = 0.5 \text{ nm}^{-1}$  and  $y = \text{relative lever length} \times 6 \text{ (nm)}$ . The dependence of force on lever arm was then calculated at each relative lever length by substituting Eq. 2 into Eq. 1 (see Fig. 4A).

## RESULTS AND DISCUSSION

To assess the role that LCs play in myosin's capacity to generate force and motion, the properties of myosin having only one of its two LCs present were determined. Myosin heavy chain, devoid of both classes of LCs, was prepared from chicken pectoralis skeletal muscle myosin (Fig. 2, lane 1). To this LC-deficient myosin (lane 2), either RLC (lane 3), ELC (lane 4), or both LCs (TLC-myosin, lane 5) were added back. As shown previously in the motility assay (4), RLC-deficient myosin and ELC-deficient myosin exhibited greater than 50% and 80% reductions in sliding velocity, respectively, when compared with either native or TLC-myosin (Table 1).

Here the effect of LC removal on myosin force production was determined with the technique described by Kishino and Yanagida (6). A single actin filament, attached to a glass microneedle, is allowed to interact with a myosin-coated surface (Fig. 3A; see *Materials and Methods*). The maximal force per unit length of actin differed among the myosins tested (Table 1; Fig. 3B). Force production by RLC-deficient myosins was unchanged when compared with that by native myosin (Table 1; Fig. 3B), but ELC removal resulted in >50% reduction in force. When ELCs were added to ELC-deficient myosin previously adhered to the nitrocellulose surface, >60% recovery of force and velocity was achieved (Table 1; Fig. 3B *Inset*). Thus, ELC can rebind to the denuded neck

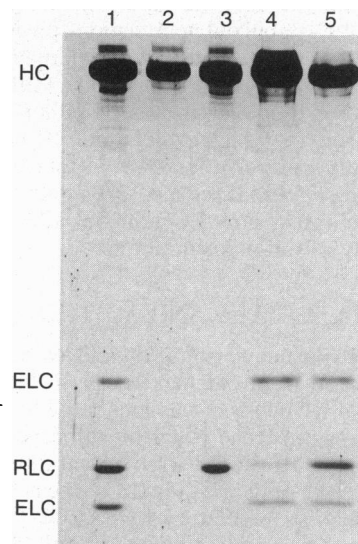


FIG. 2. SDS/12.5% PAGE of native myosin (lane 1), LC-deficient myosin (lane 2), and myosin reconstituted with either RLC (lane 3), ELC (lane 4), or both RLC and ELC (lane 5). The two ELCs are isoforms, commonly known as LC1 (upper ELC) and LC3 (lower ELC). HC, heavy chain.

Table 1. Myosin isometric force, velocity, ATPase activity, and duty cycle

Myosin	Isometric force, pN/ $\mu$ m	Velocity,* $\mu$ m/s	ATPase, <sup>†</sup> %	Duty cycle, <sup>‡</sup> %
Native	12.2 $\pm$ 1.5 <sup>§</sup>	6.9 $\pm$ 0.9	135 (3)	3.8 $\pm$ 0.5 <sup>¶</sup>
TLC	14.6 $\pm$ 2.7	6.1 $\pm$ 1.1	100 (4)	3.6 $\pm$ 0.3
RLC-deficient	11.8 $\pm$ 1.0	2.5 $\pm$ 0.6	70 (2)	4.2 $\pm$ 0.3
ELC-deficient	5.4 $\pm$ 0.9 <sup>  </sup>	1.3 $\pm$ 0.2	76 (4)	2.6 $\pm$ 0.4
Reconstituted on surface**	9.0 $\pm$ 1.0	3.9 $\pm$ 0.8		

Force is the slope and SD of its estimate for the linear regressions in Fig. 3B. Although estimates for the absolute average crossbridge force can be obtained if one knows the surface density of myosin (5, 9), relative differences can be appreciated through comparisons of the force per unit length actin in contact with the surface. There is no *a priori* reason to assume that the various myosins interact differentially with respect to the surface and/or actin (4, 5).

\*Analysis of variance was performed with a Bonferroni adjustment for multiple comparisons (13). Velocities for all reconstituted myosins were significantly different from one another ( $P < 0.05$ ).

<sup>†</sup>Average of ( $n$ )  $V_{max}$  determinations of the actin-activated ATPase activity relative to TLC-myosin, including data from ref. 4. Similar studies with soluble fragments showed that the actin-activated ATPase activity of a skeletal S1 motor domain devoid of the neck region and associated light chains was indistinguishable from that of S1 (G.S.W. and S.L., unpublished observations).

<sup>‡</sup>The crossbridge duty cycle estimate and its SD were obtained from the fit of the data in Fig. 4B.

<sup>§</sup>Data from ref. 5.

<sup>¶</sup>Data from ref. 9.

<sup>||</sup>Forces were statistically compared through multiple comparisons of the 95% confidence limits for the slopes of the linear regressions. Force generation by ELC-deficient myosin was significantly less than that by all other myosins ( $P < 0.05$ ).

\*\*Data for myosins that were reconstituted by adding ELCs back to ELC-deficient myosin previously adhered to the nitrocellulose surface.

region, and the decrease in isometric force and velocity for ELC-deficient myosin cannot be attributed to an altered adherence of this myosin to the nitrocellulose surface. Native myosin and TLC-myosin generated similar forces and velocities, confirming that the procedure for removing and then adding back the LCs did not affect myosin's force or motion-generating capacity (Table 1; Fig. 3B).

Are there structural or molecular mechanisms that can account for the differential effects of LC removal on actin filament velocity and myosin force generation? Myosin undergoes a series of mechanical and biochemical transitions as it interacts with actin to generate motion and hydrolyze MgATP. LC removal could therefore alter myosin's structure and/or the transition rates between intermediate states. We have addressed these possibilities by (i) developing a simple mechanistic crossbridge model that is both quantitative and predictive and (ii) estimating the unloaded duty cycle in the motility assay as a means of assessing changes in the kinetics of the crossbridge cycle.

Several investigators have suggested that myosin's working stroke is the result of a small conformational change in the globular, motor domain which is then amplified by the effective "lever arm," created by the neck region (3, 14, 15). If LC removal destabilizes the underlying  $\alpha$ -helix and effectively reduces myosin's lever arm length, then profound consequences to force and motion generation would be predicted (see *Lever Arm Model*). However, the predictions are valid only if LC removal does in fact shorten myosin's neck region and if the denuded neck region does not introduce a highly compliant region within the myosin molecule. In rotary-shadowed images, the characteristic pear-shaped appearance for the intact scallop myosin head becomes

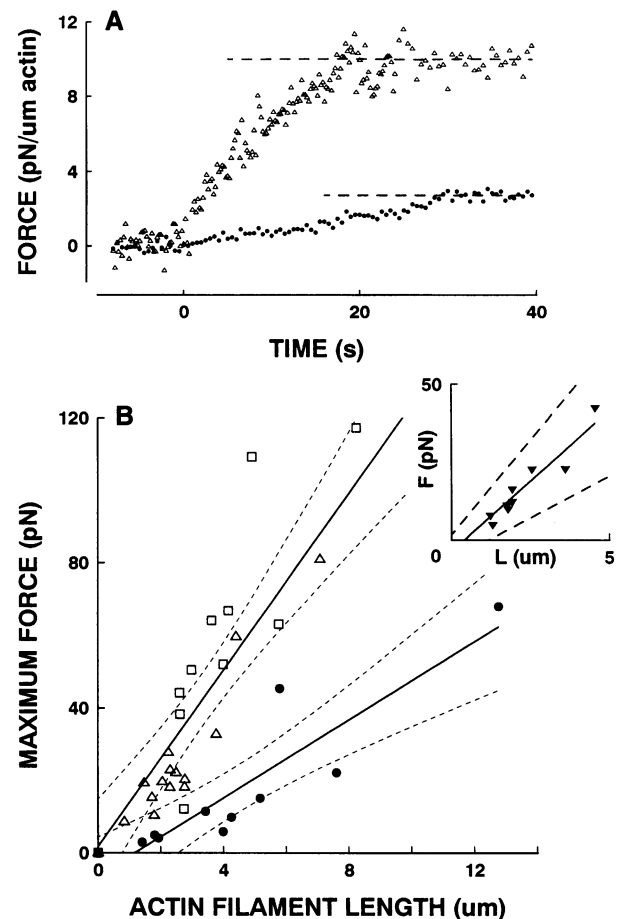


FIG. 3. (A) Time course of individual force traces is normalized to actin filament length in contact with RLC-deficient ( $\Delta$ ) and ELC-deficient ( $\bullet$ ) myosin-coated surfaces. Horizontal dashed lines indicate the steady-state maximum isometric force attained and is the force value used to construct the force vs. actin filament length plot in B. (B) Maximal force versus actin filament length in contact with myosin-coated surface for TLC-myosin ( $\square$ ) and RLC-deficient ( $\Delta$ ) and ELC-deficient ( $\bullet$ ) myosins. For comparison to all myosins tested, the linear regression (slope, 12.2 pN/ $\mu$ m) and 95% confidence limits (upper solid and dashed lines, respectively) for native myosin are plotted (data from ref. 5). The lower regression and confidence limits are for ELC-deficient myosin (slope, 5.4 pN/ $\mu$ m). Inset shows the linear regressions described above for native and ELC-deficient myosins (upper and lower dashed lines, respectively). Addition of ELCs to ELC-deficient myosin on the motility surface resulted in a significant increase in force ( $\blacktriangledown$ ) with the linear regression line shown (solid line; slope, 9.0 pN/ $\mu$ m). F, force; L, length.

smaller and rounder after RLC removal, presumably due to shortening of the neck (16). Furthermore, the denuded neck region appears to retain structural rigidity, since active stiffness was unchanged in skinned skeletal muscle fibers following partial RLC removal (17).

Based on a simple lever arm model, actin filament velocity under unloaded conditions is directly dependent on the lever's length (Figs. 1 and 4A). Since the length of  $\alpha$ -helix that is stabilized by both the RLC and the ELC is approximately equal, then removal of either LC should effectively reduce the lever arm length by approximately half. If this occurs, then a 50% decrease in the myosin step size—and thus in actin filament velocity—is predicted. This reduction in velocity was in fact observed for RLC-deficient myosin and for a genetically engineered *Dictyostelium* myosin II which lacks the binding site for RLC (18). In contrast, a 50% reduction in the myosin lever would be predicted to have little effect on the average crossbridge force.

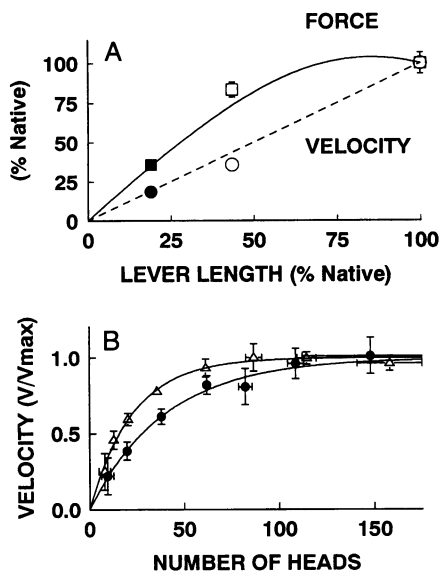


FIG. 4. (A) Lever arm model predictions for maximum average force (solid curve) and maximum actin filament velocity (dashed line) as a function of lever arm length. Changes in lever arm length, average force, and velocity are relative to native myosin. The observed average forces (squares) and velocities (circles) for RLC-deficient (open symbols) and ELC-deficient (filled symbols) myosin, relative to TLC-myosin, were best fitted to the model responses by minimizing the total error for both average force and velocity as a function of lever length. Note that the dependence of average force on lever length is similar to the T2 relationship observed by Huxley and Simmons (11). (B) Actin filament velocity versus number of ELC-deficient (●) and RLC-deficient (△) myosin heads available to interact with the actin filament. To estimate the crossbridge duty cycle, the data were fitted to a stochastic equation (solid lines; see *Materials and Methods*). Duty cycles, determined as a parameter of this fit, are given in Table 1. Velocity is normalized to the asymptote ( $a \times V_{\max}$ ) for each myosin. Each data point is the mean (with 95% confidence limits shown by bars) for an average of 30 points.

To understand how such a large change in lever arm length would have no effect on isometric force (Figs. 1 and 4A), we must rely on our adaptation of the Huxley and Simmons crossbridge model (ref. 11; see above for details). In this model, the force ( $F_{\text{avg}}$ ) for a crossbridge population would be related both to the proportion of attached crossbridges that have undergone the force-generating transition and to the extent to which an elastic element within the crossbridge is stretched during the transition. Since the extent of stretch is a linear function of lever arm length, a decrease in lever arm length would decrease the maximum force that a single crossbridge could generate (i.e., decreased  $F_{\text{uni}}$ ). However, in this case a greater proportion of attached crossbridges may undergo the working stroke (i.e., increased  $n_2$ ), thus counterbalancing the decreased force produced by each crossbridge (Fig. 4A). In agreement with this model, no effect on isometric force was observed with RLC-deficient myosin (Table 1; Fig. 3B). Partial removal of the RLC in skinned skeletal muscle fibers also showed no effect on force, although the velocity of shortening decreased in maximally activated fibers (19).

If RLC and ELC stabilize equal lengths of the neck region, then removal of either LC should similarly affect myosin's mechanics if no other factors are operative. This was not the case, since ELC removal caused larger reductions in both force and velocity than did RLC removal. Therefore for ELC-deficient myosins other mechanisms must be involved, given that an 80% reduction in lever arm length would be required if a simple lever mechanism were to be invoked (Fig. 4A). Since such a substantial reduction in the  $\alpha$ -helical neck

region seems unlikely, a more plausible explanation may be that ELC removal alters the rates at which myosin attaches to and detaches from actin (20).

To address this question, we measured the unloaded duty cycle for the LC-deficient myosins in the motility assay (9, 10), since this parameter is sensitive to alterations in the rates of crossbridge attachment and detachment (9, 10, 20). Only myosins deficient in ELC exhibited a significant change in duty cycle compared with native myosin (Table 1; Fig. 4B). This result suggests that altered crossbridge kinetics exist under unloaded conditions, which may account in part for the altered mechanical properties for ELC-deficient myosin. These observed effects on myosin's mechanical and kinetic properties are independent of small decreases in the steady-state actomyosin ATPase activity (Table 1).

## CONCLUSIONS

A simple lever arm model with its effect on isometric crossbridge distributions can account for the mechanical data obtained upon RLC removal, but this model cannot reasonably explain the effects of ELC removal. In fact, ELC removal appears to alter the kinetics of the crossbridge cycle. This does not, however, preclude a reduced lever arm as a contributing factor. Therefore, the inability to explain the effects of both RLC and ELC removal through a common molecular mechanism suggests that these two classes of LCs do not merely stabilize the neck region of myosin but may serve substantially different roles in skeletal muscle myosin's force and motion generation. A major difference between the two LCs lies in the ELC's proximity to myosin's motor domain, where the amino terminus of the myosin heavy chain abuts the ELC (3). This close interaction is reflected by the fact that MgATP hydrolysis in the motor domain caused a fluorophore bound to the ELC to decrease its signal with the same kinetics as the hydrolysis step (21, 22). It is therefore not too surprising that ELC removal in turn affects the mechanical and kinetic properties of the myosin head.

In a recent study, the entire neck region and rod were removed from a genetically engineered *Dictyostelium* myosin II (23). The resulting motor-domain fragment had a markedly increased ATPase activity, and although it did retain the ability to generate force and move actin filaments, the normalized force per molecule for the truncated head was  $\approx 30\%$  less than that for recombinant S1. Although the investigators (23) believed this difference to be insignificant, the apparent trend toward reduced forces with removal of the neck region is consistent with our findings.

It must be emphasized that the analysis presented here does not exclude alternative models. However, our model does offer testable predictions regarding the myosin step size and unitary force which are now measurable parameters, as recently described (24–26). In addition, with further development of these techniques (24, 25), stiffness measurements on a single myosin molecule may address whether or not LC removal introduces a highly compliant region to the crossbridge. This would test the adequacy of the model's assumptions and predictions. Combining biophysical and molecular biological techniques will help further our understanding of the molecular mechanisms governing the mechanical properties of such a complex molecule as myosin.

We thank Hugh Huxley for his comments on the manuscript and William Guilford, Donald Dupee, and the University of Vermont Muscle Club for their helpful discussions. This work was supported by funds from the National Institutes of Health (HL45161 and AR42231 to D.M.W. and AR17350 to S.L.) and from the Muscular Dystrophy Association. K.M.T. is an Established Investigator of the American Heart Association.

1. Huxley, H. E. (1969) *Science* **164**, 1356–1366.
2. Cooke, R. (1986) *CRC Crit. Rev. Biochem.* **21**, 53–118.
3. Rayment, I., Rypniewski, W. R., Schmidt-Base, K., Smith, R., Tomchick, D. R., Benning, M. M., Winkelmann, D. A., Wessenberg, G. & Holden, H. M. (1993) *Science* **261**, 50–58.
4. Lowey, S., Waller, G. S. & Trybus, K. M. (1993) *Nature (London)* **365**, 454–456.
5. VanBuren, P., Work, S. S., & Warshaw, D. M. (1994) *Proc. Natl. Acad. Sci. USA* **91**, 202–205.
6. Kishino, A. & Yanagida, T. (1988) *Nature (London)* **334**, 74–76.
7. Warshaw, D. M., Desrosiers, J. M., Work, S. S. & Trybus, K. M. (1990) *J. Cell Biol.* **111**, 453–463.
8. Work, S. S. & Warshaw, D. M. (1992) *Anal. Biochem.* **202**, 275–285.
9. Harris, D. E. & Warshaw, D. M. (1993) *J. Biol. Chem.* **268**, 14764–14768.
10. Uyeda, T. Q. P., Kron, S. J. & Spudich, J. A. (1990) *J. Mol. Biol.* **214**, 699–710.
11. Huxley, A. F. & Simmons, R. M. (1971) *Nature (London)* **233**, 533–538.
12. Reedy, M. K., Holmes, K. C. & Tregear, R. T. (1965) *Nature (London)* **207**, 1276–1280.
13. Kleinbaum, D. G., Kupper, L. L. & Muller, K. E. (1988) *Applied Regression Analysis and Other Multivariable Methods* (PWS-Kent, Boston), p. 362.
14. Huxley, H. E. & Kress, M. (1985) *J. Muscle Res. Cell Motil.* **6**, 153–161.
15. Vibert, P. & Cohen, C. J. (1988) *J. Muscle Res. Cell Motil.* **9**, 296–305.
16. Flicker, P. F., Wallimann, T. & Vibert, P. (1983) *J. Mol. Biol.* **169**, 723–741.
17. Hofmann, P. A., Metzger, J. M., Greaser, M. L. & Moss, R. L. (1990) *J. Gen. Physiol.* **95**, 477–498.
18. Uyeda, T. Q. P. & Spudich, J. A. (1993) *Science* **262**, 1867–1870.
19. Moss, R. L., Giulian, G. G. & Greaser, M. L. (1982) *J. Biol. Chem.* **257**, 8588–8591.
20. Huxley, A. F. (1957) *Prog. Biophys. Biophys. Chem.* **7**, 255–318.
21. Marsh, D. J. & Lowey, S. (1980) *Biochemistry* **19**, 774–784.
22. Marsh, D. J., Stein, L. A., Eisenberg, E. & Lowey, S. (1982) *Biochemistry* **21**, 1925–1928.
23. Itakura, S., Hisashi, H., Toyoshima, Y. Y., Ishijima, A., Kojima, T., Harada, Y., Yanagida, T., Wakabayashi, T. & Sutoh, K. (1993) *Biochem. Biophys. Res. Commun.* **196**, 1504–1510.
24. Finer, J. T., Simmons, R. M. & Spudich, J. A. (1994) *Nature (London)* **368**, 113–119.
25. Ishijima, A., Harada, Y., Kojima, H., Funatsu, T., Higuchi, H. & Yanagida, Y. (1994) *Biochem. Biophys. Res. Commun.* **199**, 1057–1063.
26. Miyata, H., Hakozi, H., Yoshikawa, H., Suzuki, N., Kinoshita K., Jr., Nishizaka, T. & Ishiwata, S. (1994) *J. Biochem. (Tokyo)* **115**, 644–647.